Proc. Natl. Acad. Sci. USA
Vol. 88, pp. 561–564, January 1991
Biochemistry

X-ray scattering indicates that the leucine zipper is a coiled coil

(GCN4/eukaryotic transcription/peptide model/three-dimensional structure)

RANDY RASMUSSEN[†], DOMINIC BENVEGNU[†‡], ERIN K. O'SHEA[§¶], PETER S. KIM[§‖], AND TOM ALBER[†,††]

[†]Department of Biochemistry, University of Utah School of Medicine, Salt Lake City, UT 84132; [§]Whitehead Institute for Biomedical Research, 9 Cambridge Center, Cambridge, MA 02142; Departments of [¶]Chemistry and [‖]Biology, Massachusetts Institute of Technology, Cambridge, MA 02139; and [††]Department of Chemistry, University of Utah, Salt Lake City, UT 84112

Communicated by Gerald R. Fink, October 8, 1990

ABSTRACT **Dimerization of the bZIP class of eukaryotic transcriptional control proteins requires a sequence motif called the leucine zipper. We have grown two distinct crystal forms of a 33-amino acid peptide corresponding to the leucine zipper of the yeast transcriptional activator GCN4. This peptide is known to form a dimer of parallel helices in solution. X-ray scattering from both crystal forms shows reflections that are diagnostic of coiled coils. The most notable reflections occur at ≈5.2 Å resolution and correspond to the pitch of helices in coiled coils. There is no diffraction maximum near 5.4 Å, the characteristic pitch of straight helices. Our results provide direct evidence that the leucine zipper of GCN4 is a coiled coil.**

The leucine zipper sequence motif (1) is known to be responsible for the dimerization of several eukaryotic transcription factors including Fos, Jun, and GCN4 (for reviews, see refs. 2 and 3). The specificity of dimer formation, and indirectly of DNA recognition, can be determined solely by interactions between the leucine zipper sequences. Peptides corresponding to the isolated leucine zipper sequences of Fos and Jun, for example, form heterodimers preferentially in a manner analogous to the intact proteins (4).

Leucine zippers were identified on the basis of heptad repeats of leucine residues (1). Four heptad repeats, together with an adjacent region rich in basic residues, are sufficient for DNA binding by the yeast transcriptional activator GCN4 (5). The leucine repeats were originally proposed to form a dimer of anti-parallel α-helices stabilized by interdigitation of leucine residues aligned on one face of each helix (1). This proposed interdigitation was the basis for naming the structure a zipper.

There is growing evidence, however, that the leucine repeat sequences are the shortest members of a well-known class of proteins that form parallel helical coiled coils. The characteristic leucine repeat, for example, occurs four residues out of phase with a second repeat of hydrophobic amino acids (6). This "4–3 hydrophobic repeat" is one of the hallmarks of parallel coiled coils (for a review, see ref. 7). More directly, synthetic peptides corresponding to the leucine zippers of GCN4 (6), Fos, and Jun (4) are found to be (*i*) α-helical as judged by circular dichroism spectroscopy, (*ii*) dimeric as determined by sedimentation equilibrium, and (*iii*) oriented in a parallel manner as judged by disulfide crosslinking. In addition, two-dimensional NMR experiments confirm that the peptide corresponding to the leucine zipper of GCN4 is helical and forms a symmetric dimer, as expected for a coiled coil (8).

Nevertheless, direct structural evidence that leucine zippers fold as coiled coils, in which the helices are bent around each other, is lacking. Straight α-helices and coiled coils differ in the location and the resolution of characteristic x-ray reflections (9–11). Thus, x-ray diffraction is well suited for distinguishing between these structures.

We report here the crystallization of a peptide, referred to as GCN4-p1, that corresponds to the GCN4 leucine zipper (6). We show that the x-ray diffraction patterns of two distinct crystal forms have features similar to the scattering observed from a parallel coiled-coil protein, α-keratin. One crystal form is suitable for determination of the structure of GCN4-p1 at high resolution.

MATERIALS AND METHODS

Peptide Synthesis and Crystallization. The peptide GCN4-p1 (*N*-acetyl-RMKQLEDKVEELLSKNYHLENEVARLKKLVGER) was synthesized and purified as described (6). Twinned hexagonal plates of GCN4-p1 were grown at room temperature by vapor diffusion of peptide solutions (20 mg/ml) containing 10 mM $NaPO_4$, 0.15 M NaCl, and 0.02% NaN_3 at pH 7.0 against 50% (wt/vol) ammonium sulfate (Schwarz/Mann, Ultrapure). Monoclinic crystals were obtained by vapor diffusion of the peptide (10–20 mg/ml) in 25 mM $NaPO_4$/0.4 M NaCl at pH 7–7.8 against 15% polyethylene glycol 1200 (Sigma). Polyethylene glycols with molecular weights ranging from 1000 to 8000 all induced crystal growth.

X-Ray Data Collection and Analysis. Crystals were mounted in sealed capillaries (Charles Supper, Natick, MA) directly from the crystallization drops, because no stabilizing synthetic mother liquor was found. To record the diffraction pattern of α-keratin, a quill of the North American porcupine (*Erethizon dorsatum*) was mounted in air by inserting the end into modeling clay (Crayola) on a goniometer head (Charles Supper). Still and precession photographs were recorded on an Enraf-Nonius camera using nickel-filtered copper radiation from a Rigaku RU200 rotating anode source. Three-dimensional x-ray intensities to a maximum resolution of 1.95 Å were collected on a single monoclinic crystal of GCN4-p1 by using a Rigaku AFC6R diffractometer. Intensities were determined by Lehmann–Larsen analysis of a 50-step ω scan across each peak (Molecular Structure, The Woodlands, TX). Three standard reflections were measured repeatedly to monitor and correct for radiation damage. The intensities of the corrected standards varied by <3%. Lorentz and polarization corrections, as well as an empirical absorption correction (12), were applied during data processing.

The positions of the noncrystallographic two-fold rotation axes were determined by using the MERLOT program package (13). In brief, the product of the rotated and unrotated Patterson syntheses was evaluated as a function of rotation

The publication costs of this article were defrayed in part by page charge payment. This article must therefore be hereby marked "*advertisement*" in accordance with 18 U.S.C. §1734 solely to indicate this fact.

[‡]Present address: Department of Cell Biology, Stanford University School of Medicine, Stanford, CA 94305.

angles, ϕ, φ, and κ. This product has a high value only when the rotated and unrotated Patterson functions are highly correlated. A two-fold rotation axis is specified by $\kappa = 180°$, and ϕ and ψ are the polar angles that specify the position of the two-fold axis. In a right-handed coordinate system with a^* initially parallel to y and b^* initially parallel to z, $+\phi$ is a counterclockwise rotation about z, $+\psi$ is a counterclockwise rotation about the new y, and κ is a rotation about the new z. X-ray data from 7 to 3 Å resolution and 5° steps of ϕ and ψ were used.

RESULTS

To establish the overall structure of the GCN4-p1 dimer, we compared the x-ray diffraction patterns of the peptide with the diffraction pattern of α-keratin, a classic coiled-coil protein. Because x-ray diffraction maxima arise from repeated elements of structure, similar diffraction patterns provide strong evidence for conformational similarity.

Precipitation of GCN4-p1 with ammonium sulfate yielded twinned hexagonal plates. The peptide molecules are arranged in a trigonal or hexagonal lattice with unit cell dimensions $a = b = 34.5$ Å, $c = 51.8$ Å (Fig. 1). Because a 33-residue helix would be ≈50 Å long, the helices are likely to be aligned along the c axis. This conclusion is supported by the strong reflections at ≈10 Å resolution (Fig. 1 *A* and *B*) expected from the side-to-side packing of helices.

In a helical coiled coil, the helices are bent, and the rise per turn is ≈5.15 Å [compared to a rise per turn of 5.4 Å in a straight α-helix (9–11, 14–18)]. These structural features produce diagnostic reflections in the diffraction patterns of coiled-coil proteins. To measure the helical repeat distance in GCN4-p1, a 9.8° screenless precession photograph was recorded perpendicular to the helix direction (Fig. 1*B*). This precession angle (corresponding to a resolution limit of 4.5 Å in the *h*0*l* zone) allows the repeat to be visualized even if the helices are tilted up to 10° from the c axis in the crystal. The most striking features in this photograph are the strong reflections at 5.15 to 5.2 Å resolution on or near the 00*l* (vertical) axis. These reflections are absent in 3° precession photographs (data not shown), as expected for helices aligned with the c axis. The 5.15 to 5.2 Å reflections, then, stem from the helical repeat reinforced by the unit cell spacing. Also as expected for a coiled coil (9–11, 14–18), streaks crossing the 00*l* axis at 5.0 Å resolution are seen in 3° and 9.8° (Fig. 1*B*) screenless precession photographs of the *h*0*l* setting.

These features in the diffraction pattern of the hexagonal crystal form of GCN4-p1 are characteristic of x-ray scattering from parallel coiled coils (refs. 9–11, 14–18 and Fig. 1*C*). The *h*0*l* zone of the hexagonal crystal form of GCN4-p1 contains reflections analogous to the meridional reflections of α-keratin at 5.15 Å resolution, the near meridionals at 5.0 Å resolution, and the equatorial reflections at 10 Å resolution (Fig. 1*C*). Significantly, GCN4-p1 gives no diffraction maxima straddling the 00*l* axis at 5.4 Å resolution, which would be characteristic of straight α-helices (9, 10).

A second crystal form of GCN4-p1 that diffracts x-rays to at least 2 Å resolution was grown by using polyethylene glycol as the precipitant. Precession photographs show that the crystals have the symmetry of the monoclinic space group $C2$ with $a = 101.7$ Å, $b = 30.5$ Å, $c = 21.9$ Å, and $\beta = 94.7°$ (Fig. 2). There is a peptide dimer in the asymmetric unit [$V_m = 2.1$ Å^3 per dalton (19)].

The overall distribution of x-ray scattering from the monoclinic crystal form is also similar to the diffraction pattern of α-keratin. As shown in Fig. 2, strong reflections consistent with the side-to-side packing of helices occur near 10 Å resolution. In an orthogonal direction corresponding to scattering from the helical repeat, the strongest reflections occur at spacings less than 5.3 Å resolution (Fig. 2*B*). These dominant spacings in the direction of the superhelix axes almost certainly reflect the helical repeat of the peptide molecules themselves, because similar spacings are observed when the molecules are packed in two different crystal lattices.

The superhelix axis of a parallel coiled coil coincides with a two-fold rotation axis of symmetry. Consequently, we compared the locations of the superhelix axes in the monoclinic crystals of GCN4-p1 with the locations of noncrystallographic two-fold symmetry axes. The superhelix axes of the GCN4-p1 dimers are in or near the a–c plane inclined ≈27° from the a axis. This conclusion is supported by the restrictions on packing the ≈50 Å-long dimers in the unit cell and the characteristic reflections noted above in the *h*0*l* precession photograph (Fig. 2*A*). By using the MERLOT program package (13), two noncrystallographic two-fold rotation axes were found at $\phi = 60°$, $\psi = 90°$ and $\phi = -30°$, $\psi = 90°$. The first axis is equivalent to the superhelix axis of the dimer: this finding is consistent with a parallel coiled-coil structure. The

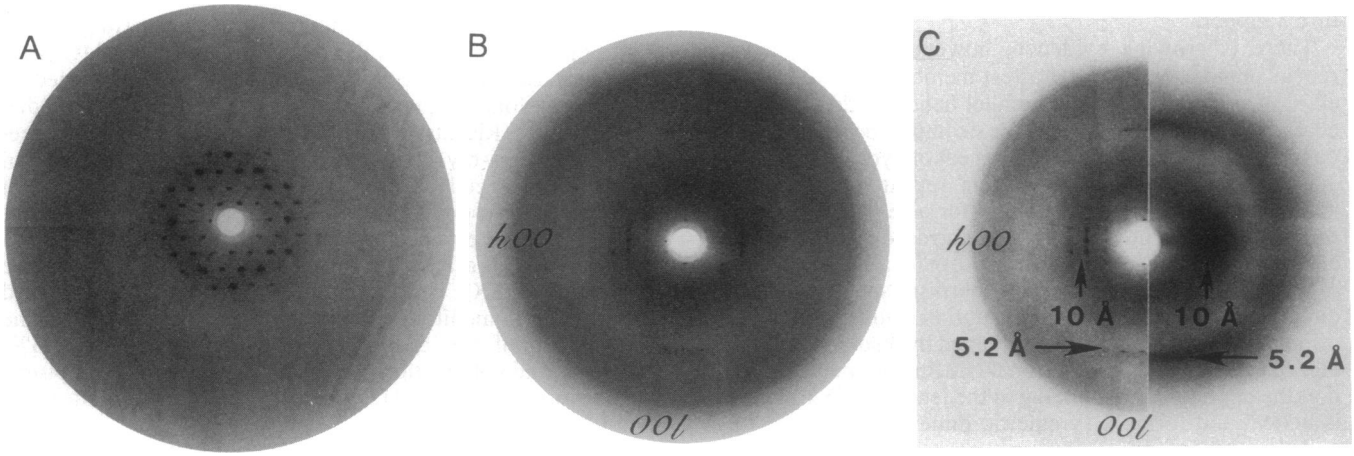

FIG. 1. Screenless 9.8° precession photographs of the *hk*0 (*A*) and *h*0*l* (*B*) settings of hexagonal crystals of GCN4-p1. The unit cell dimensions are $a = b = 34.5$ Å and $c = 51.8$ Å. Overall, the diffraction pattern extends to ≈6.5 Å resolution in the hexagonal plane (*A*) but only to ≈26 Å resolution along the 00*l* axis (*B*). In the *h*0*l* zone (*B*), strong reflections also occur close to the 00*l* axis at 5.18 Å resolution, and near-axial streaks occur at 5.0 Å resolution. (*C*) Composite of the *h*0*l* precession photograph and a still diffraction photograph of keratin recorded from the tip of a quill of the North American porcupine (*Erethizon dorsatum*). Spacings on the *h*00 axis (equator) and the 00*l* axis (meridian) are indicated. The spacings in the two halves of *C* do not align precisely due to the different geometries of precession and still photographs.

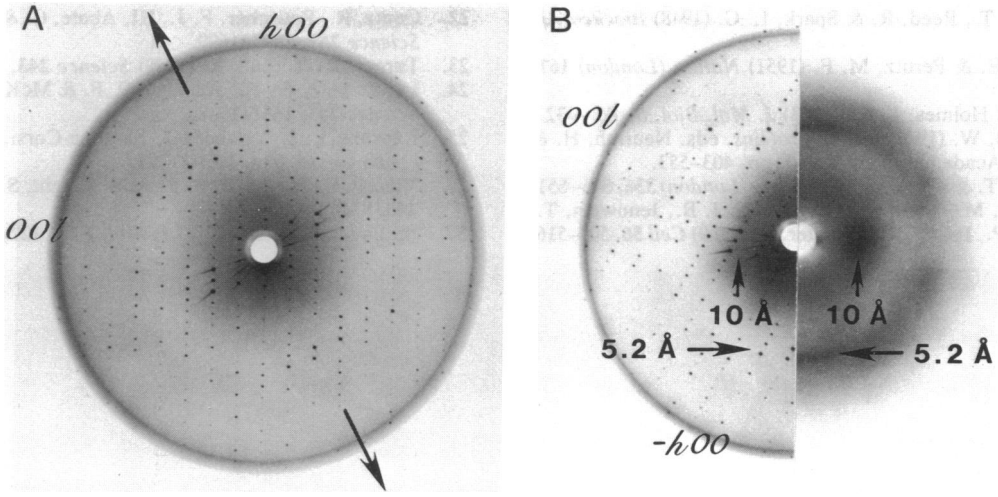

FIG. 2. (*A*) Precession photograph (17°) of the *h0l* zone of the monoclinic crystals of GCN4-p1. Together with precession photographs of the *hk*0 (17°) and 0*kl* (15°) zones (provided for review), this diffraction pattern indicates that the crystals have the symmetry of space group *C*2 with unit cell dimensions $a = 101.7$ Å, $b = 30.5$ Å, $c = 21.9$ Å, and $\beta = 94.7°$. The helical repeat gives rise to the strongest reflections between 4.8 and 5.5 Å resolution in a three-dimensional x-ray data set—namely, the 14,0,3 (at 4.91 Å resolution) and the 16,0,2 (at 5.27 Å resolution) present in this photograph. These occur in a direction perpendicular to strong reflections near 10 Å resolution (e.g., the −2,0,2; −2,0,3; and −2,0,4) expected from the side-to-side packing of helices. (*B*) Comparison of the *h0l* zone with the diffraction pattern recorded from the tip of a quill of the North American porcupine. Diagnostic distances in the two patterns are marked. Strong reflections in the *h0l* zone in the direction of the superhelix axis correspond to spacings less than 5.3 Å.

second axis is perpendicular to the first and arises from the symmetry of the Patterson function.‡‡

DISCUSSION

The x-ray diffraction pattern of a coiled coil of helices differs from that of paired straight helices in two diagnostic ways (9–11): reflections arising from the helical repeat occur on the meridian (instead of displaced from the meridian) and at 5.15 to 5.2 Å resolution (rather than at 5.4 Å resolution). These features, which are prominent in the diffraction pattern of α-keratin, are also evident in the diffraction patterns of two crystal forms of GCN4-p1 (Figs. 1*C* and 2*B*). Thus, x-ray scattering provides direct evidence that the leucine zipper of GCN4 forms a short coiled coil.

In a parallel coiled coil, equivalent leucines in adjacent helices make side-to-side contacts with each other (as in a handshake), rather than being interdigitated. In the direction of the superhelix axis, the leucine pairs are adjacent to two pairs of residues in the alternate hydrophobic position of the heptad repeat (see figure 5 of ref. 6). Our finding that the superhelix axis in the monoclinic crystal form of GCN4-p1 is equivalent to a noncrystallographic two-fold rotation axis of symmetry, together with the earlier finding that the GCN4-p1 monomers associate in a parallel manner (6), demonstrates that the helices are in register and are not interdigitated or displaced from each other.

As noted previously (6, 20–26), dimerization of transcription factors through a parallel coiled-coil motif can facilitate recognition by placing the DNA-binding regions next to each other in space. In addition, the superhelical twist of the commonly observed four or five heptad repeats would cause a rotation of about 90° between the DNA-binding basic region and the structures at the opposite end of the coiled coil (9, 11, 14, 27). Thus, the length of the leucine repeat region, which is conserved among leucine zipper proteins, could determine the relative orientations of different transcription factor domains and thereby establish the orientation of transcription factor complexes with respect to DNA.

High-resolution structural studies, required to understand the specificity of dimer formation, are made possible by the monoclinic crystal form described here. Because there is no detailed structure available for any two-stranded parallel coiled coil, the structure of GCN4-p1 also will be particularly useful for detailed modeling of natural and designed coiled-coil proteins.

‡‡Strictly speaking, the possibility that the monomers are related by the second noncrystallographic two-fold axis (at $\phi = -30°$, $\psi = 90°$) cannot be ruled out. This interpretation seems much less likely, however, because it would require that adjacent dimers pack more tightly (along the 22 Å *c* axis) than monomers within each dimer (along the 30 Å *b* axis). Moreover, this alternative interpretation would require that the helices within the dimer pack in an antiparallel manner, in contrast to crosslinking studies indicating that the parallel dimer is at least 1000-fold more stable than the antiparallel dimer (6).

We thank R. Rutkowski for peptide synthesis, T. Oas for helpful discussions, P. Fitzgerald for the MERLOT programs, and B. R. Marley for collecting porcupine quills. E.K.O. is a Howard Hughes Medical Institute Doctoral Fellow. This work was supported by grants from the National Institutes of Health (GM-44162 to P.S.K.), the Lucille P. Markey Charitable Trust (to P.S.K.), and the American Cancer Society (MV-382 to T.A.).

1. Landschulz, W. H., Johnson, P. F. & McKnight, S. L. (1988) *Science* **240**, 1759–1764.
2. Mitchell, P. J. & Tjian, R. (1989) *Science* **245**, 371–378.
3. Johnson, P. F. & McKnight, S. L. (1989) *Annu. Rev. Biochem.* **58**, 799–839.
4. O'Shea, E. K., Rutkowski, R., Stafford, W. F., III & Kim, P. S. (1989) *Science* **245**, 646–648.
5. Hope, I. A. & Struhl, K. (1986) *Cell* **46**, 885–894.
6. O'Shea, E. K., Rutkowski, R. & Kim, P. S. (1989) *Science* **243**, 538–542.
7. Cohen, C. & Parry, D. A. D. (1986) *Trends Biochem. Sci.* **11**, 245–248.
8. Oas, T. G., McIntosh, L. P., O'Shea, E. K., Dahlquist, F. W. & Kim, P. S. (1990) *Biochemistry* **29**, 2891–2894.
9. Crick, F. H. C. (1952) *Nature (London)* **170**, 882–883.
10. Crick, F. H. C. (1953) *Acta Crystallogr.* **6**, 639–689.
11. Crick, F. H. C. (1953) *Acta Crystallogr.* **6**, 689–697.
12. North, A. C. T., Phillips, D. C. & Mathews, F. S. (1968) *Acta Crystallogr.* **24**, 351–359.
13. Fitzgerald, P. M. D. (1988) *J. Appl. Crystallogr.* **21**, 273–278.
14. Pauling, L. & Corey, R. B. (1953) *Nature (London)* **171**, 59–61.
15. MacArthur, I. (1943) *Nature (London)* **152**, 38–41.

16. Astbury, W. T., Reed, R. & Spark, L. C. (1948) *Biochem. J.* **43,** 282–287.
17. Huxley, H. E. & Perutz, M. F. (1951) *Nature (London)* **167,** 1053–1054.
18. Cohen, C. & Holmes, K. C. (1963) *J. Mol. Biol.* **6,** 423–432.
19. Matthews, B. W. (1977) in *The Proteins*, eds. Neurath, H. & Hill, R. L. (Academic, New York), pp. 403–553.
20. Kouzarides, T. & Ziff, E. (1988) *Nature (London)* **336,** 646–651.
21. Schuermann, M., Neuberg, M., Hunter, J. B., Jenuwein, T., Ryseck, R.-P., Bravo, R. & Müller, R. (1989) *Cell* **56,** 507–516.
22. Gentz, R., Rauscher, F. J., III, Abate, C. & Curran, T. (1989) *Science* **243,** 1695–1699.
23. Turner, R. & Tjian, R. (1989) *Science* **243,** 1689–1694.
24. Landschulz, W. H., Johnson, P. F. & McKnight, S. L. (1989) *Science* **243,** 1681–1688.
25. Ransone, L. J., Visvader, J., Sassone-Corsi, P. & Verma, I. M. (1989) *Genes Dev.* **3,** 770–781.
26. Vinson, C. R., Sigler, P. B. & McKnight, S. L. (1989) *Science* **246,** 911–916.
27. McLachlan, A. D. (1978) *J. Mol. Biol.* **122,** 493–506.